Modeling of friction in cold forging considering a wide range of tribological conditions

C. Hu[1,2], S. Volz[1], P. Groche[1], P. Moreau[3], J. Launhardt[1], N. Benabbou[3], S. Saito[4], H. Chen[2], K. Kitamura[4], L. Dubar[3]

[1]*Institut for Production Engineering and Forming Machines, Technical University of Darmstadt, Darmstadt, Germany*
[2]*Institute of Forming Technology & Equipment, School of Material Science and Engineering, Shanghai Jiao Tong University, Shanghai 200030, China*
[3]*University of Valenciennes and Hainaut Cambresis — LAMIH UMR CNRS 8201 Carnat Arts Institute. France*
[4]*Department of Electrical and Mechanical Engineering, Nagoya Institute of Technology, Japan*

Corresponding author: Peter Groche, peter.groche@ptu.tu-darmstadt.de

The work introduced in this contribution is the result of an international collaborative research initiated by the ICFG subgroup "Lubrication". Four students from different institutes in Europe and Asia contributed to it. The friction coefficients in cold forging were determined by four different tribometers. A wide range of tribological conditions was recreated. The derived data was used to model friction in cold forging with the aid of mathematical fitting and machine learning algorithms. The presentation will reveal the established procedure of collaboration as well as results of experiments and mathematical modeling.

Friction modelling; cold forging; mathematical fitting; machine learning

1. Introduction

In cold forging processes, the workpiece is deformed under high pressure resulting in material flow at the interface between the workpiece and the die, causing large friction forces in opposing direction to the relative movement between the workpiece and the die. Friction is a very complex physical phenomenon, which affects the material flow, the forming load, the surface quality of the workpiece, and the service life of the dies. A general friction model was furtherly confirmed by experimental and numerical investigations into the upsetting of a semi-tapered specimen [1]. The Coulomb friction law and the constant shear friction law were compared using a rigid-plastic finite element method, and considerable differences existing in simulation results can be observed between the two friction laws [2]. Different friction models generate different friction stress distributions, and it can be found that calibration curves of the friction area ratio are more sensitive to friction [3]. Based on compression-twist testing results, a mathematical model was established for friction as a function of normal pressure and tool/workpiece interface temperature [4]. Another friction model considering the sliding velocity between tools and the workpiece was developed [5]. A critical normal pressure was defined between the Coulomb friction law at low normal pressures and the constant friction model at high normal pressures [6], and a new law of friction involved with the effect of the ratio of real contact area under oil-lubricated condition was proposed [7]. As reviewed by Nielsen and Bay, during the last 80 years, most important contributions on theoretical models of friction in metal forming are based on the analysis of the real contact area and different understandings of asperity flattening in tool-workpiece interfaces [8].

In tribological systems of metal forming, the tribological loading conditions can mainly be described with four quantitive parameters including contact normal stresses, surface expansion ratio, relative sliding velocity between tool and workpiece and initial temperature [9]. There are relatively large differences between the empirically determined friction coefficients from different tribometers, but it can be well explained when the respective tribological loads are considered [10]. Against this background a friction model for metal forming can be created, considering the relationship between tribological loads and friction force. In this work, four tribometers were used to measure friction forces for a wide range of tribological conditions, typically occurring in cold forging. The collected data is used to create different friction models, using mathematical fitting and machine learning algorithms, to linking the tribological loads and the coefficient of friction.

2. Material flow curves and extrapolation

All specimens used during tribometer testing were produced by turning using a single batch of cold-rolled 16MnCr5 steel that has previously been soft annealed. Flowcurves were determined using compression tests at RT, 100°C, 200°C, 300°C, 400°C with strain rates of $\dot{\varphi}$ = 0.1 and 1. In order to account for high strain, the flowcurves were extrapolated using a combination of voce and swift equation with a factor α that controls the weight between both parts, as shown in Equation (1). The α was defined as 0.3, all other parameters in Equation (2) were determined by the method of minimum mean square error using the experimental data. The specific values are calculated and recorded in Table 1.

$$k_f = \alpha \cdot swift + (1-\alpha) * voce \quad (1)$$

$$k_f = \alpha \cdot (s_1 \cdot (s_2 + \varphi)^{s_3}) + (1-\alpha) * (v_1 + (v_2 - v_1) \cdot e^{-v_3 * \varphi} \quad (2)$$

Table 1 Material model parameters

Temperature	Strain Rate	Voce - Parameters			Swift - Parameters			α
		v_1	v_2	v_3	s_1	s_2	s_3	0.3
RT	0.1	757	421	8.416	810	0.000551	0.1167	0.3
100 °C	0.1	713	427	5.342	739	-0.0042	0.1157	0.3
200 °C	0.1	665	362	5.813	697	0.000102	0.1325	0.3
300 °C	0.1	675	382	5.013	701	0.000377	0.1327	0.3
400 °C	0.1	629	353	8.487	663	0.000238	0.1057	0.3
RT	1	748	440	10.950	787	-0.0039	0.0848	0.3
100 °C	1	692	407	8.145	727	0.000236	0.1019	0.3
200 °C	1	666	367	5.540	697	0.000582	0.1325	0.3
300 °C	1	671	363	4.930	698	0.000222	0.1425	0.3
400 °C	1	620	356	8.543	650	0.000386	0.1003	0.3

As shown in Figure 1, the flowcurves were extrapolated to a large strain of 4 according to the combined swift-voce model with determined parameters in Table 1. The flowcurves were used for all finite element models of the tribometer tests.

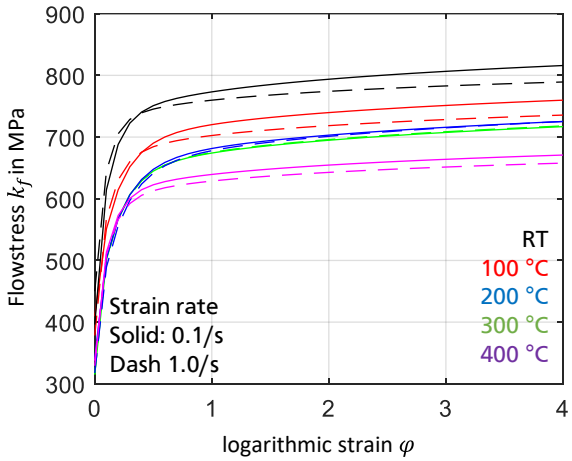

Figure 1 Extrapolated flowcurves of 16MnCr5 steel

3. Tribometers and tribological conditions

In this experimental work, four tribometers were used. The Ring Compression Test with Boss (RCT-B) was developed to overcome the disadvantages of the conventional ring compression test. By measuring the dimensional change of the outer diameter and the height of the specimen the Coefficient of Friction (COF) can be determined through a comparison with a group of calibration curves based on simulation results [11]. In principle, the Contact Normal Pressure (CNP) and Surface Expansion Ratio (SER) can be changed by variation of the height reduction, and the Relative Sliding Velocity (RSV) can be adjusted using different forming speeds. The Backward Can Extrusion Test (BCET) was developed based on a backward can extrusion operation with a reduction in cross-sectional area of around 50%. The COF is determined based on the assumption, that the pull-back force is proportional to the COF. The COF can therefore be determined by directly measuring the pull-back force of the punch after the backward extrusion [12]. In the Upsetting Sliding Test (UST) [13], a convex indenter is upset into the specimen to induce the desired CNP and a partially deformed state, before sliding at a defined velocity and distance is carried out. The normal and the tangential forces are measured during the sliding process, allowing the calculation of the COF, by e.g. the Amontons-Coulombs friction law. The Sliding Compression Test (SCT) devides the deformation (compression) and the sliding process into two sequential steps. In the compression step, the nominal compression force can be adjusted to the desired value of CNP and SER. During the sliding step the normal and the tangential forces are logged by piezoelectric load cell while the RSV can be adjusted. Based on the measured forces, the COF can be directly calculated [14]. The SCT offers a high flexibility and a good control of the tribological loads during testing. Loads can be kept constant over the duration of testing allowing the measurement of the friction force at defined, constant tribological loads.

Due to the individual characteristics of the tribometers, each test offers different flexibility and a possible range of tribological loads. A single tribometer test often doesn't allow the measurement of COFs for the entire range of tribological loads typically

occurring in cold forging whereas the combination of four different tribometers allows the determination of COFs for a much wider range of tribological loads. Based on the typical spectrum of loads occurring in cold forging and the characteristics of the four tribometers the testing conditions were defined, according to Table 2.

Table 2 Defined tribological conditions of different tribometers

Tribometer	RCT-B	BCET	UST	SCT
Contact Normal Stress, CNS (MPa)	800-1000	1700-2000	1200-1600	1600-2000
Surface Expansion Ratio, SER	1.0-2.0	9.0-35.0	1.1	3.0-11.0
Relative Sliding Velocity, RSV (mm/s)	0.3-50.0	40.0-100.0	50.0-100.0	100.0-250.0

Identical lubrication and surface treatment were applied to all specimen by Nihon Parker Ltd., Japan. All surfaces were wetblasted prior to the application of the lubricant. The lubricant was applied by 60 s dipping followed by 600 s drying in an oven. The lubricants main components are polymer, wax and salt. No conversion layer such as zinc phosphate was used.

Previous collaborative, global tribometer tests within the ICFG subgroup lubrication showed that single layer lubrication systems, such as the one used within this test are sensitive to packaging, shipping and storage conditions. When specimens are sent between Europe, Japan and China multiple times for production, lubrication and testing, long custom handling and shipping times as well as rough transportation conditions can occur. In order to decrease the impact of these factors all specimens where individually, tightly packed and exclusively sent via airmail. This ensures short transportation times and prevents the lubrication from damaging during travel. Furthermore, the different tribometer tests in China, Japan, France and Germany where all carried out at a similar time after lubricant application in Japan in order to prevent possible aging effect, caused by long storage and handling times.

4. Results, modelling and discussion

4.1 Results

In Figure 2(a) the tribological loads of the different tests are plotted. Multiple loads change simultaneously between the tests while the parameter of surface expansion ratio is relatively less involved than the other two parameters. Correspondingly, the determined average value of COF in each test is plotted on Figure 2(b). It can be seen, that the COF depends on the tribological loads. Furtherly, a simplified analysis about the influence of single tribological loads can be carried out with Figure 2(c) and Figure 2(d). In general, the COF decreases with an increasing RSV. At small values of RSV, close to static friction, the COF increases to values up to 0.09. This trend is in accordance with multiple past investigations [15,16]. An increase in CNP often leads to a decrease in COF [17,18], which can be confirmed within this study, where lower CNP for RCTB lead to relatively large COFs. At the range of 1200 MPa to 1600

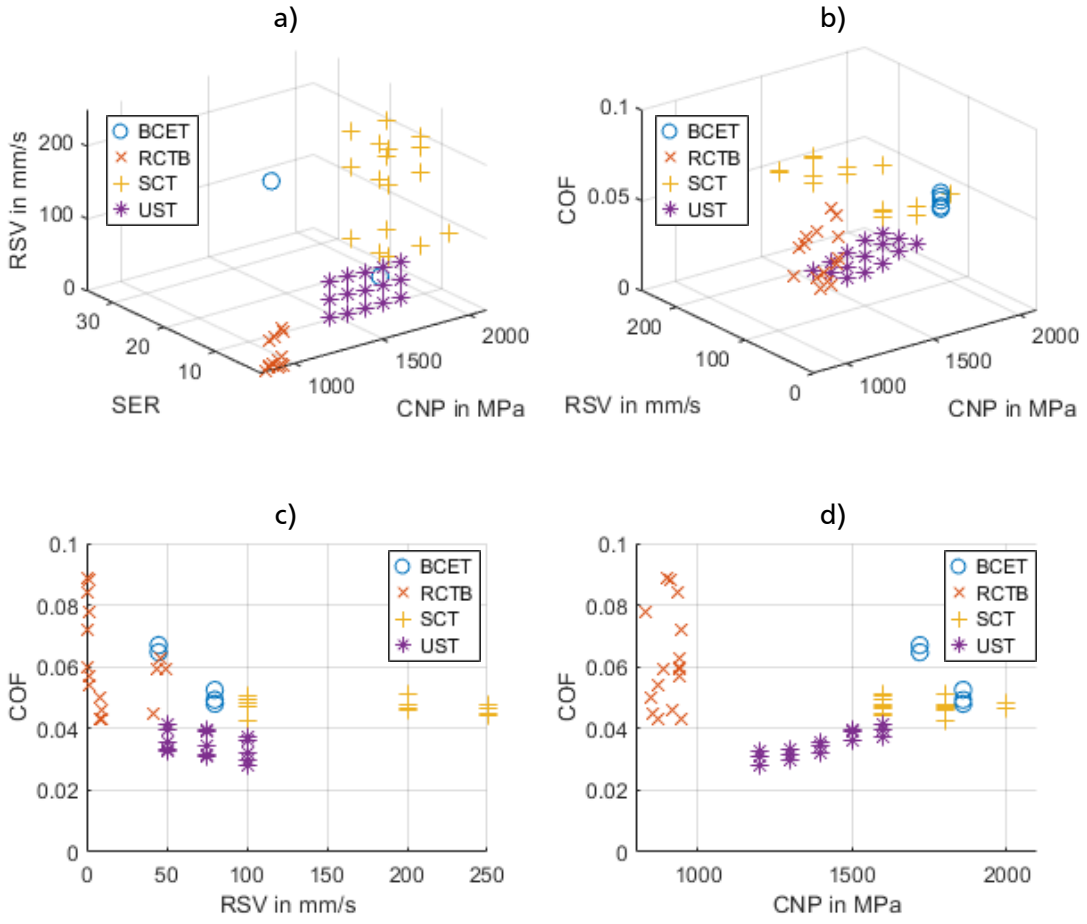

Figure 2 tribological loads and experimental results

MPa where COFs where measured by UST, the COFs are relatively smaller. This can likely be explained by two contributing factors, where very low SER values occur during UST, putting little strain on the lubrication system and large differences in the interface temperature due to different deformation degrees of the tribometer tests.

4.2 Modelling

Friction modelling plays a significant role in the accuracy of FEM simulation of metal forming processes. While it is often industrial practice to assume a constant COF, various past investigations measuring COFs at different tribological loads have repeatedly shown that the COF is strongly dependent on the tribological loads acting in the contact zone. Depending on the forming process a significant improvement of the accuracy of FEM simulation can be achieved through implementation of advanced friction models paying respect to the various influencing factors. As shown in Fig. 2, the COF of the used lubricant is strongly dependent on the tribological loads. In the following chapter, different analytical models and machine learning approaches are applied to the experimental data.

The experimental data is divided into training data and test data. The training data consists of 80% of the data and is used to derive the model parameters. The test data consisting of 20% of the data is used to evaluate the quality of the derived model. During testing, the model is used to predict the COF of the test data which is then compared to the true values of the test data. The typical logarithmic regression, and more advanced machine learning approaches such as a support vector regression or artificial neural network (ANN) are adopted. The error between the modelling prediction and the experimental data gives information on the quality of the model.

Assuming a logarithmic link between the tribological loads and the COF, the following analytical Equation (3) can be created by the logarithmic regression.

$$\mu = c_1 + c_2 \cdot \ln(\sigma_n) + c_3 \cdot \ln(v_{rel}) + c_4 \cdot \ln(\psi) \tag{3}$$

The derived constant parameters are: $c_1 = 0.113$, $c_2 = -0.01027$, $c_3 = -0.0004813$, $c_4 = 0.007618$. The constant parameters c_2 and c_3 are negative, and these show the inverse proportional relationship between the CNP, RSV and the COF. The logarithmic regression model can well reflect the influence of tribological loads on the COF.

The residual plot of the logarithmic regression showing the measured COF (true values) and the difference between the predicted value and the true value (residue) for both, the training and the testing data (see Figure 3). The root square mean error (RSME) during testing is 0.008417, the mean absolute error (MAE) = 0.006656 and R^2 = 0.5472. A residue of 0 corresponds with a perfect prediction of the analytic model, where the true value and the predicted value are identical. The overall quality of the prediction of the logarithmic model is good with a low MAE of 0.006656. The residual plot reveals a weak prediction bias where the residue corresponds with the true value meaning that for low true values the predicted COF is too high and for high COFs the predicted COF is too low.

Figure 3 Residue plot of logarithmic regression

The support vector regression algorithm has the characteristics of simple structure and high classification accuracy. Even in the case of a small sample size, it can obtain better statistical results. As present in Figure 4, the support vector regression shows similar prediction quality as the logarithmic regression. The coefficient of determination R^2 value is higher than that of logarithmic value with a more pronounced prediction bias towards higher true COFs.

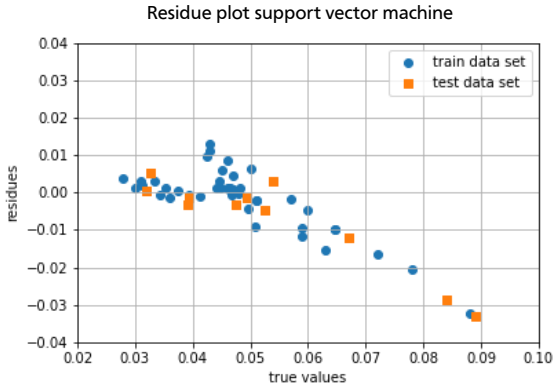

Figure 4 Residue plot of support vector regression

ANN are suitable for modelling of complex problems especially when the system interdependencies are nonlinear. A neural network is trained to predict the COF based on the tribological loads. The hyperparameters of the neural network, like the structure, the initial learning rate, and the activation functions, were determined with a Bayesian optimization. The initial learning rate was set to 0.01 which decreases exponentially with an increasing number of training epochs. The input layer consists of three input neurons: CNP, RSC and SER. The output layer consists of a single output neuron – the COF. The first hidden layer consists of 100 neurons with a tangens hyperbolicus activation function. The second hidden layer consists of 15 neurons using a tangens hyperbolicus activation function. The training of the ANN takes 30 epochs and is terminated due to an implemented early-stopping criterion. The ANN has an RMSE during testing of 0.008535. The Residue plot of the ANN is similar to the support vector regression with a prediction bias for true values > 0.05, as shown in Figure 5(b).

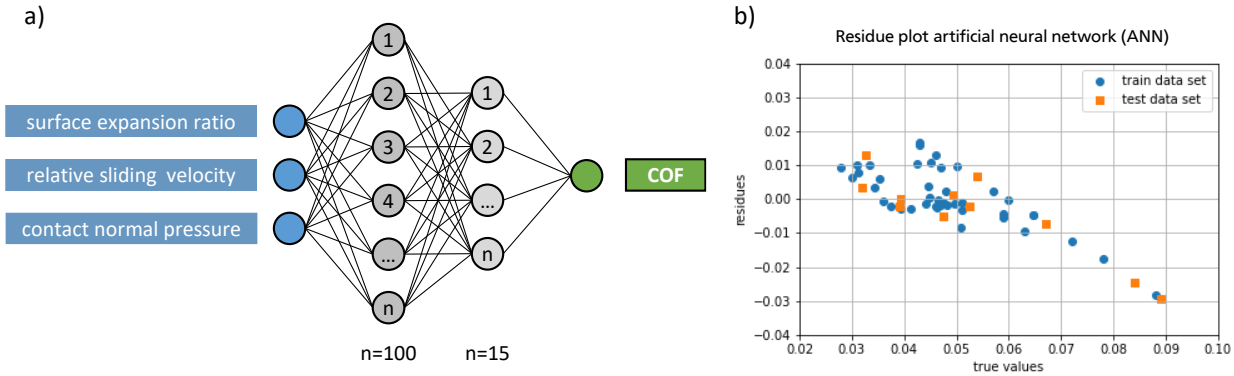

Figure 4 Structure(a) and residue plot(b) of the artificial neural network

Figure 6 shows the residues of different modelling methods. The distribution of the residue of the logarithmic regression is between -0.04~0.04, the range is the smallest. The RMSE of the logarithmic regression is 0.008417, and it is smaller than that of the other methods, as recorded in Table 3. However, the MAE and RSQ of the logarithmic regression are relatively larger. In general, the prediction accuracy of different models is not very high, but the prediction accuracy of the model created by the logarithmic regression is the best. In this modelling process, the relationship between tribological load and friction coefficient can be expressed by the logarithmic regression based on mathematical fitting. However, the accuracy is limited on the assuming relationship. The relatively poor prediction accuracy of the support vector regression and ANN is probably caused by a too small set of data of current tests.

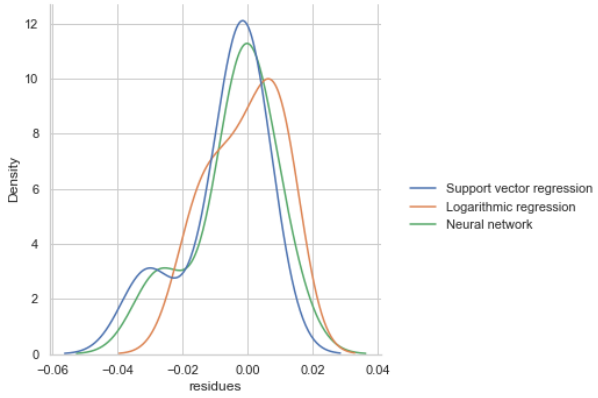

Figure 5 Comparison of residues probability distribution for all models

Table 3 Comparison of model error values

Model Name	RMSE	MAE	RSQ
Logarithmic Regression	0.008417	0.006655	0.5472
Support Vector Regression	0.008541	0.005541	0.5338
Artificial Neural Network	0.008535	0.006261	0.5345

5. Summary and Outlook

Within this work different tribometer tests where used to measure the COF over a wide range of tribological loads. Four universities from Japan, France, Germany and China worked together within the framework of the International Cold Forging Group (ICFG), subgroup “lubrication” to coordinate the experimental work in a collaborative student work. A single batch of16MnCr5 was used for the production of all specimens used within this work. The same set of flowcurves, derived from compression tests, extrapolated with a combined Swift-Voce approach, were used for all FE-simulations. Surface treatment and lubrication with a single

layer lubricant was applied identically for all specimens by Nihon Parkerizing Co. LTD., Japan. Previous testing revealed that single layer lubricants are sensitive to rough shipping conditions, long shipping duration and toll handling times. Therefore, all specimens were firmly and individually packed, shipped simultaneously using air mail to ensure prompt delivery with low impact on the lubrication quality.

All tribometer results where combined to a single set of data, consisting of 57 data points containing the COF and the corresponding tribological loads. The data was used to fit mathematical models and to train different machine learning approaches in an effort to evaluate different approaches to model the tribological system. The models used within this work are: logarithmic regression, support vector regression and an artificial neural network. The data was split into 80 % training and 20 % testing data. The relatively poor performance of the machine learning approaches is likely caused by a too small data base and gaps within the tribological loads that were tested. Furthermore, differences in COF for the same tribological loads are observable between different tribometers. This is likely due to differences in the contact temperature caused by differences in the deformation degree of the tribometer tests. Tests such as the UST have a low deformation degree, generating only little heat in the contact zone, while tests such as the BCET cause large temperatures in the contact zone due to larger deformation.

While within the presented work, the logarithmic regression and the ANN show the best model quality. Machine learning algorithms such as ANNs are overall a promising approach to model the complex interdependencies in the tribological system. Future investigations will focus on creating a larger data base by using direct tribometer tests such as the SCT. This allows a much larger database which will enhance the quality of a ANN. Future investigations will additionally focus on expanding the ANN to more input neurons including important factors such as the contact temperature, surface conditions, material, etc. and the integration of the trained model into FEM Simulations, determining the COF on nodal levels for each increment according to the tribological loads acting in the contact zone.

Acknowledgement

The authors gratefully acknowledge the financial support for the international logistics cost from International Cold Forging Group and the continuous support of all members of the Subgroup “Lubrication”. Special thanks to Dr. Shinobu Komiyama and Nihon Parkerizing Co. LTD., Japan for their support of this particular study. The first author would like to thank the Alexander von Humboldt Foundation for the support of the research on tribology in metal forming.

References

[1] Petersen, S.B., Martins, P.A.F. and Bay, N., Friction in bulk metal forming: a general friction model vs. the law of constant friction. Journal of Materials Processing Technology, 1997. 66(1-3): 186-194.
[2] Joun, M.S., Moon, H.G., Choi, I.S., Lee, M.C. and Jun, D.B., Effects of friction laws on metal forming processes. Tribology International, 2009. 42(2), pp.311-319.
[3] Tan, X., Comparisons of friction models in bulk metal forming. Tribology International, 2002, 35(6): 385-393.
[4] Bay, N., Eriksen, M., Tan, X. and Wibom, O., A friction model for cold forging of aluminum, steel and stainless steel provided with conversion coating and solid film lubricant. CIRP annals, 2011, 60(1): 303-306.
[5] Behrens, B.A., Bouguecha, A., Hadifi, T. and Mielke, J., Advanced friction modeling for bulk metal forming processes. Production Engineering, 2011, 5(6): 621-627.
[6] Wang, Z.G., Yoshikawa, Y., Suzuki, T. and Osakada, K., Determination of friction law in dry metal forming with DLC coated tool. CIRP Annals, 2014, 63(1): 277-280.
[7] Wang, Z.G., Dong, W.Z. and Osakada, K., Determination of friction law in metal forming under oil-lubricated condition. CIRP Annals, 2018, 67(1): 257-260.
[8] Nielsen, C.V. and Bay, N., Review of friction modeling in metal forming processes. Journal of Materials Processing Technology, 2018, 255: 234-241.
[9] Bay, N., Azushima, A., Groche, P., Ishibashi, I., Merklein, M., Morishita, M., Nakamura, T., Schmid, S. and Yoshida, M., Environmentally benign tribo-systems for metal forming. CIRP annals, 2010, 59(2): 760-780.
[10] Groche, P., Kramer, P., Bay, N., Christiansen, P., Dubar, L., Hayakawa, K., Hu, C., Kitamura, K. and Moreau, P., Friction coefficients in cold forging: A global perspective. CIRP Annals, 2018, 67(1): 261-264.
[11] Hu, C., Ou, H. and Zhao, Z., An alternative evaluation method for friction condition in cold forging by ring with boss compression test. Journal of Materials Processing Technology, 2015, 224: 18-25.
[12] Asai, K., Kitamura, K., Goto, K. and Hayashi, N., Estimation of frictional coefficient between punch and billet at back-stroke in backward can extrusion test of steel. In Key Engineering Materials, 2018, 767: 248-255.
[13] Lazzarotto, L., Dubar, L., Dubois, A., Ravassard, P. and Oudin, J., Identification of Coulomb's friction coefficient in real contact conditions applied to a wire drawing process. Wear, 1997, 211(1): 54-63.
[14] Groche, P., Stahlmann, J. and Müller, C., Mechanical conditions in bulk metal forming tribometers—Part two. Tribology International, 2013, 66: 345-351.
[15] Groche, P.; Zang, S.; Müller, C.: Einfluss der Relativgeschwindigkeit auf tribologische Systeme der Kaltmassivumformung, Heft 61, S. 26–32. 2013
[16] Stribeck, R.: Die wesentlichen Eigenschaften der Gleit- und Rollenlager. Zeitschrift des Vereins Deutscher Ingenieure 46 (1902), 1341-1470
[17] Groche, P., Stahlmann, J., Hartel, J. and Köhler, M., 2009. Hydrodynamic effects of macroscopic deterministic surface structures in cold forging processes. Tribology International, 42(8), pp.1173-1179.
[18] Kraus, M.; Lenzen, M.; Merklein, M.: Contact pressure-dependent friction characterization by using a single sheet metal compression test. Wear 476 (2021), S. 203679